



Geochemical characteristics of carbonate rocks in a salinized lacustrine basin: a case study from Oligocene formation in the Qaidam Basin, northwestern China

Qilin Chen¹ · Daowei Zhang² · Jianguo Wang¹ · Fan Zhao^{1,2} · Yingru Liu¹ · Zhenggang Zhang¹ · Xiujian Sun¹ · Chenggang Huang¹ · Yadong Bai¹

Accepted: 31 January 2020 / Published online: 12 March 2020
© Springer-Verlag GmbH Germany, part of Springer Nature 2020

Abstract

Based on petrology, mineralogy, carbon and oxygen isotope composition, trace element composition, geochemical characteristics of carbonate rocks are systematically analyzed in the saline lacustrine basin environment in the Qaidam Basin, northwestern China. The results show that: (1) The carbon and oxygen isotopic compositions show carbonate rocks were deposited between open lake and closed lake environment; (2) the Sr/Ba ratio is greater than 1 with an average of 2.01; the Sr/Cu ratio is greater than 5 with an average of 109.04; the U/Th average value ratio is less than 1 with an average of 0.62. These data indicated the carbonate rocks deposited in an salinization, drought, and reducing lacustrine environments; (3) Σ REE values range from 39.41 to 162.67 ppm with an average of 87.67 ppm, and negative anomaly of Eu occurs in REE distribution patterns; and (4) lithologies of carbonate rocks are mainly composed of dark gray or black carbonates, commonly associated with salts deposition due to different lacustrine facies.

Keywords Geochemical characteristics · Salinized lacustrine basin · Carbonate rocks · Stable carbon and oxygen isotopes

Introduction

Lacustrine carbonate rocks refer to the carbonate rocks formed in the inland lake basins, including carbonate rocks deposited in fresh water (Zhao 2013), in brackish water–saline water and in salt lakes. The lacustrine carbonate rocks are not only regarded as important source rocks, but also as important reservoir rocks (Peng 2011; Zhou et al. 1991; Tuo et al. 1995; Tuo and Huang 1996). Numerous oil and gas reservoirs have been widely discovered in the lacustrine carbonate rocks.

Qaidam Basin, one of the continental petroliferous basins in northwestern China, is an important component of Tibetan Plateau (Fig. 1). The Qaidam basin is a typically foreland basin on the northeastern margin of the Tibet Plateau (Zhu

1986; Jia 2005). Based on drilling data, the Qaidam basin has undergone two complete Tectonic evolution, since the Mesozoic and these tectonic movements resulted in three sedimentary strata sequences. Depocenter of the basin in Paleogene was formed in the Western Qaidam Basin, then gradually migrated eastward. Depocenter of saline lacustrine sedimentary basins is not only controlled by tectonic evolution but also by the late tectonic pattern and distribution. Neogene stratigraphy is subdivided into six sets of bottom-up land Formation (Table 1).

Lacustrine carbonate rocks are obviously controlled by the changes in the paleoclimate, fossil water force and fossil water medium conditions. Paleoclimate influence is much greater in lakes than in the oceans (Xia et al. 2003; Zhao 2014). Due to location at the aggregation and intersection area in China, the climatic system in the Qaidam Basin, can sensitive to the Asian climate change, even to the global climate change (Mao et al. 2014). Lacustrine carbonate rocks was selected to study petrologic features and reservoir conditions in the Qaidam Basin to determine controlling factors and formation mechanism of lacustrine carbonate rock reservoirs.

✉ Fan Zhao
fan_zh2002@163.com

¹ Research Institute of Petroleum Exploration and Development-northwest, Lanzhou 730020, China

² PetroChina Qinghai Oilfield Company, Dunhuang 736202, China

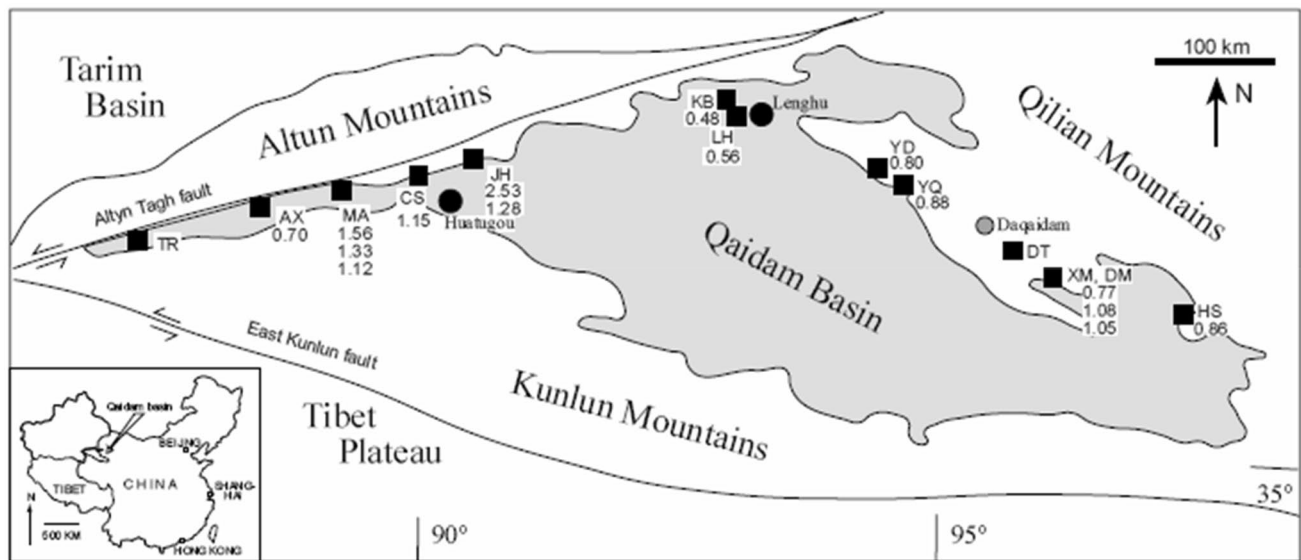


Fig. 1 Study objects Location map of Qaidam Basin

Table 1 Mesozoic and Cenozoic Chronostratigraphic framework in western Qaidam basin

| Ara | Age | Epoch | Formation | Code |
|------------------|------------------|----------------|-----------------------------|------------------|
| Cenozoic | Quaternary | Holocene | hubuxun | Q ₄ |
| | | Pleistocene | Qigequan | Q ₁₊₃ |
| | | Neogene | Pliocene | Shizigou |
| | Upper Youshashan | | N ₂ ² | |
| | Lower Youshashan | | N ₂ ¹ | |
| | Miocene | | Upper Gancaigou | N ₁ |
| | Paleogene | Oligocene | Lower Gancaigou | E ₃ |
| | | Eocene | Lulehe | E ₁₊₂ |
| | | Mesozoic | Cretaceous | Late Cretaceous |
| Early Cretaceous | Quyagou | | | K ₁ |
| Jurassic | Late Jurassic | | Hongshigou | J ₃ |
| | | | Chaishiling | |
| | Mid Jurassic | | Dameigou | J ₂ |
| | | | Xiaomeigou | |
| Early Jurassic | Huxishan | J ₁ | | |

Samples and methods

The core samples are selected from Yuejin area, Yingxi area, Ganchaigou area and Xianshuiquan area in the Qaidam Basin (Table 1) (Yin et al. 2007). The technical methods mainly include thin section observation, X-ray diffraction analysis, total rock mineral contents, scanning electron microscope (SEM), and electronic probe. All of above mentioned analysis and tests were carried out in the Key Laboratory of Reservoir Description, CNPC.

The thin section observation was conducted on thickness of 0.03 mm using the Zeiss Axio Scope A1 polarizing microscope.

The X-ray diffraction analysis were ground into powder with grain sizes less than 40 μm . The power was weighed to make a test piece by backpressure method, and the integrated intensities of diffraction peaks for individual minerals were measured. Total rock mineral contents in percentage were calculated, the instrument model was Empyrean. During the analysis, the working voltage was 40 kV, the current was 40 mA, the scanning speed was 2° (2 θ)/min, and the sampling step width was 0.02° (2 θ).

The scanning electron microscope were cut into cubes or irregular bulks with a 1 cm³ volume. The fresh sections were selected as the observation surfaces, and the conductive metallic element Au was coated onto the surfaces. The conducting resin was used to fix the samples onto the sample holder, and the observation surfaces were connected with the sample holder for the electric charges conduction. In addition, the instrument model was FEI Quanta 450 FEG during the analysis with the working voltage of 20 kV and the electron incident flow of 3×10^{-10} – 4×10^{-10} A.

The dolomite composition analysis was obtained by electronic probe, under an working voltage of 15 kV using a working current of 25 μA . The spot size was 5 μm , and the testing time at each probe point was about 2 h. The detected element composition included MgO, CaO, Na₂O, Al₂O₃, SiO₂, K₂O, MnO, FeO, SrO and BaO.

For stable carbon and oxygen isotopes, core samples and phosphate were mixed together in sample tube to react after vacuumizing for half an hour at 72°C. Liquid nitrogen and cold trap (about -196 °C) were used to collect carbon dioxide

gas. Purify it and make it enter the mass spectrometer analysis and testing, correction according to the standard sample (GBW04405) and the standard unit (V-PDB), the carbon and oxygen stable isotope error is no more than 0.1‰ based on repeating the test.

Results and discussion

Sedimentary characteristics

As the exploration deepens in each exploration phase, a lot of previous research achievements made one same conclusion: the Oligocene stratum is the most important hydrocarbon source rocks in the entire Qaidam Basin. Based on the analysis of 109 dark mudstones and carbonate rocks, it is indicated that the average organic carbon content ranges from 0.3 to 2% with an average of 0.77%. Most samples have moderate abundances of organic matter, and the hydrocarbon conversion rate is relatively high in salinization. Therefore, strong hydrocarbon generation capacity for oil source rocks occurs in each area of the Qaidam Basin.

In view of the overall color of rocks, lithology is dominated by dark colors such as dark gray or gray black, with no oxidation or weak oxidation colors. Although fine-grained terrigenous clastic stripes can be occasionally observed in strata, this cannot be considered as necessary and sufficient conditions to classify the lake basin as shore-shallow lacustrine due to relatively shallow water depth. The reason for this is that the contents of terrigenous clastics in the lacustrine facies carbonate rock strata mainly depend on the attenuation index of kinetic energy of river water with clastic particles flowing into the lake, i.e., in saline water, fine-grained clastic materials can be transported much farther, while coarse-grained clastic particles flowing into the lake are subject to bigger kinetic energy attenuation because of the resistance effect.

Some scholars once questioned whether the saline minerals development will make the lake basin dry up or water depth shallow in later period? This is not the case, because the saline minerals deposition mainly depends on whether saline minerals in the lake water approach saturation point, not depends on the lake water depth. Moreover, the abundance carried minerals flowing into the lake plays a decisive role. This inference can be basically supported by a simple laboratory experiment. Use a bowl fresh water (bowl diameter 10 cm, height 6 cm) to represent relatively shallow fresh water lake, and use a saline water basin (basin diameter 40 cm, height 20 cm) to represent relatively deep saline lake. Dissolve salt (NaCl) into saline water until the water is saturated, and then leave the bowl and the basin under sunshine for continuous evaporation. The experiment results indicate that no saline minerals

precipitates can be found upon evaporation of fresh water from the bowl, whereas saline minerals are quickly precipitated at the beginning of the saline water evaporation from the basin although there is still much saline water left in the basin. The results shows that the saline minerals precipitation can also occur in semi-deep lacustrine or deep lacustrine facies provided that the saline minerals in lake water have reached their saturations, having nothing to do with the water lake depth,

Electron microprobe analysis about the actual drilling in 2017, the gypsum symbiosis was confirmed by energy spectrums of dozens of crystals with black mudstone containing calcite in strata (Fig. 2), and this proved that the saline minerals precipitation exists in deep water even without evaporation, drying up or exposure to surface.

Petrological characteristics

The whole rock mineral content analysis by XRD of drilling cores from Yuejin Area, Yingxi Area, Ganchaigou Area and Xianshuiquan Area in the Western Qaidam Basin, indicated that the carbonate contents (including dolomite and calcite) from such four areas were 69.8%, 54.6%, 45.0%, and 37.0%, respectively. The clastics contents were 11.8%, 19.2%, 27.8% and 30.6%, respectively. The shale content were 6.8%, 12.8%, 18.7% and 27.9%, respectively, and the authigenic minerals contents were, respectively, 11.7%, 13.4%, 8.6% and 4.6% (Fig. 3). The results revealed that the Yuejin area and Yingxi area had the highest carbonate contents (54.6% and 40.4% of dolomite, respectively); Xianshuiquan area and Ganchaigou area had the highest terrigenous clastics contents; Xianshuiquan area had the highest shale content; and Yingxi area had the highest saline minerals content. The rock components are closely related to the sedimentation environment. Long meandering river with sedimentary source is arrived in the east of the area-carrying abundant saline mineral solutes, such as Ca^{2+} , SO_4^{2-} , Na^+ , Cl^- , Mg^{2+} , CO_3^{2-} and a little Ba^{2+} , Sr^{2+} . This process would make important contribution to precipitation of abundant saline minerals in the Yingxi area, or aggregation certain thickness salt bed, or mineral granules in the carbonate rocks (Huang et al. 2017). Due to the lake waves and fine-grained clastic particles and shale content are sedimented in lake, resulting in relatively high abundances of terrigenous clastics and shale contents in Ganchaigou area and Xianshuiquan area in the north. The Yuejin Area is a lake-bay area with relatively shallow water bodies and algae is developed and can easily break through the dynamic barrier formed by dolomite the hydration shell on the Mg^{2+} surface (Huang et al. 2016a; You et al. 2011), which is good for dolomitization and result in the highest content of dolomite in Yuejin area (Table 2).

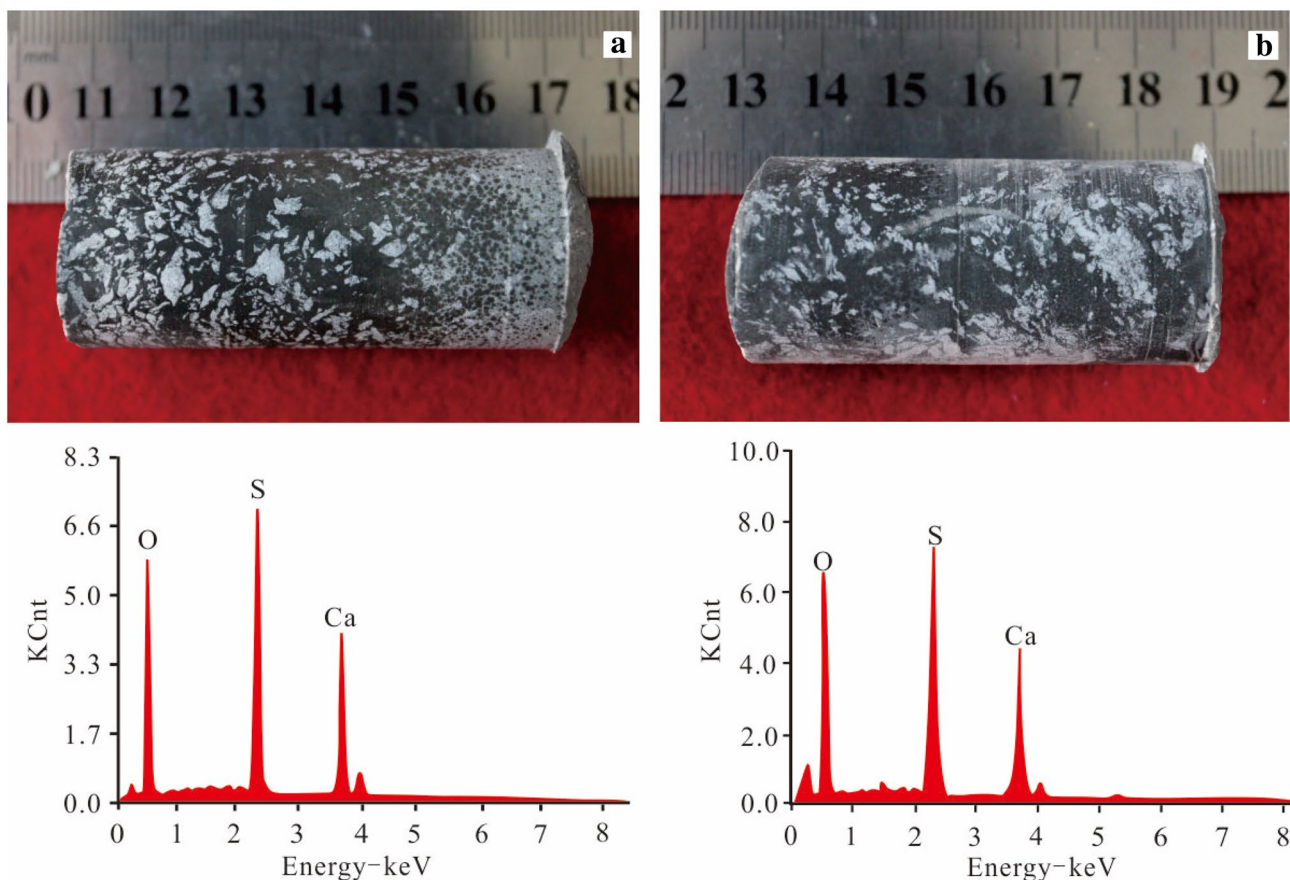
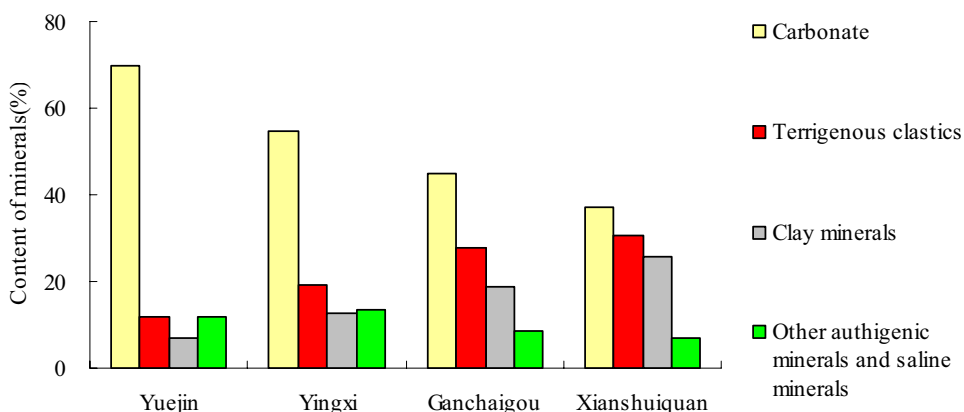


Fig. 2 Symbiosis of black containing calcite mudstone with gypsum of E₃ reservoirs of deep water deposits from Well S49-1 in the Yingxi area

Fig. 3 Comparison of rock components of Oligocene reservoirs in the Western Qaidam Basin



Carbon and oxygen isotope analysis

In the continental lake, carbon and oxygen isotopes of pro-togenetic carbonates are important indicators for ancient environment and climate change. Previous studies have shown $\delta^{18}\text{O}$ and $\delta^{13}\text{C}$ in rock that the period is new and suffer feebly late reformation are more closely related to the original sedimentary. For the samples after Mesozoic, $\delta^{18}\text{O}$ and $\delta^{13}\text{C}$ in carbonate rocks is more useful to study

depositional environment. The carbon and oxygen isotopic composition in research area suffer from alteration faintly, so it can reflect original carbon and oxygen isotopic information during depositional stage in lake water.

The variation of carbon isotopic ratio in lacustrine carbonate sediments is controlled by inorganic carbon isotope composition in the lake water, and separately effect between the dissolved inorganic carbon (TDIC) and carbonate precipitation mineral. The inorganic carbon $\delta^{13}\text{C}$ dissolved in the

Table 2 Statistical table of the whole rock mineral content analysis by XRD of main reservoirs of Oligocene in the Qaidam Basin

| Name of area | Sample no. | Depth (m) | Designation | Quartz | Potash feldspar | Plagioclase | Calcite | Dolomite | Aragonite | Siderite | Magnesite |
|-----------------|------------|-----------|---------------------------------------|--------|-----------------|-------------|---------|----------|-----------|----------|-----------|
| Yuejin area | YH101-5 | 2927.40 | Algal dolomite containing calcite | 4.9 | 0.6 | 3.2 | 19.5 | 0 | 13.3 | 6.7 | 0 |
| | YH101-16 | 2928.85 | Dolomite containing mud | 13.3 | 1.1 | 4.9 | 6.4 | 0 | 0 | 0.6 | 0 |
| | YH101-71 | 2943.05 | Dolomite containing silt | 7.7 | 0.6 | 3 | 5.7 | 0 | 0 | 0 | 0 |
| | YH101-293 | 3160.40 | Dolomite containing silt | 7.3 | 0.4 | 2.4 | 6.6 | 0 | 0 | 7.4 | 0 |
| | YH101-670 | 3208.64 | Sandy dolomite containing calcite | 8.1 | 0.3 | 4.4 | 6.7 | 0 | 0 | 5.1 | 0 |
| | YH106-2 | 3281.70 | Dolomite containing silt | 10.6 | 1.7 | 4.4 | 11.3 | 0 | 3.7 | 6.1 | 2.6 |
| | YH106-3 | 3294.20 | Dolomite | 4.6 | 0.2 | 2.2 | 7.5 | 0 | 0 | 7.0 | 0 |
| | YH106-11 | 3366.10 | Dolomite | 4.0 | 0 | 1.8 | 16.7 | 0 | 0 | 0 | 0 |
| | YH106-16 | 3358.40 | Dolomite | 6.6 | 0.3 | 2.9 | 6.6 | 0 | 0 | 0 | 0 |
| | YH106-27 | 3381.90 | Dolomite containing silt | 9.6 | 0.5 | 3.4 | 11.1 | 0 | 0 | 0.6 | 0 |
| Yingxi area | Average | | | 7.7 | 0.6 | 3.3 | 9.8 | 0.0 | 1.7 | 3.4 | 0.3 |
| | S3-1-3 | 4366.8 | Dolomite | 9.7 | 0.7 | 5.1 | 10 | 20.2 | 0 | 17.5 | 0 |
| | S3-1-7 | 4369.35 | Dolomite | 13.8 | 0.7 | 8.2 | 4.5 | 0 | 0 | 13.1 | 0 |
| | S3-1-23 | 4376.63 | Dolomite | 11.8 | 1.1 | 8.0 | 15.9 | 0 | 0 | 0 | 0 |
| | S3-1-38 | 4371.15 | Silty dolomite | 11.7 | 1.7 | 12.6 | 6.9 | 0 | 0 | 0.2 | 0 |
| | S41-6-1-10 | 3857.35 | Dolomite containing silt | 5.7 | 0.7 | 7.8 | 9.5 | 0 | 0 | 3.5 | 0 |
| | S41-6-1-11 | 3857.95 | Dolomite containing silt | 12.1 | 1.3 | 11.3 | 7.6 | 38.2 | 0 | 11.7 | 0 |
| | S41-6-1-12 | 3858.48 | Saline dolomite containing silt | 4.2 | 0.5 | 6.7 | 2.2 | 37.4 | 0 | 5.9 | 0.2 |
| | S41-6-1-22 | 3867.12 | Dolomite containing mud | 6.1 | 1.1 | 5.2 | 5.9 | 0 | 0 | 0 | 0 |
| | S38-1 | 2794.62 | Argillaceous dolomite containing silt | 14.8 | 0.9 | 6.5 | 8.4 | 16.2 | 0 | 0 | 0 |
| Ganchaigou area | S38-11 | 3147.16 | Dolomite containing calcite | 8.8 | 1.0 | 9.1 | 18.3 | 0 | 0 | 0 | 0 |
| | Average | | | 9.9 | 1.0 | 8.1 | 8.9 | 11.2 | 0 | 5.2 | 0 |
| | C6-1 | 1916.00 | Carbonate rock containing silt | 15.1 | 1.0 | 7.0 | 13.1 | 0 | 6.6 | 6.3 | 0 |
| | C6-2 | 20100 | Silty carbonate rock containing mud | 21.9 | 1.1 | 8.9 | 12.6 | 0 | 4.6 | 0 | 0 |
| | C6-3 | 2115.00 | Carbonate rock containing silt | 15.6 | 0.8 | 6.0 | 9.3 | 0 | 3.3 | 6.8 | 0 |
| | C6-4 | 2214.00 | Silty carbonate rock containing mud | 23.4 | 1.4 | 6.9 | 15.4 | 0 | 7.9 | 0.2 | 0 |
| | C6-5 | 22600 | Silty carbonate rock containing mud | 19.1 | 0.8 | 6.4 | 15.9 | 0 | 1.9 | 0 | 0 |
| | C6-6 | 2347.00 | Silty carbonate rock containing mud | 17.1 | 2.7 | 9.2 | 14.9 | 0 | 4.0 | 6.8 | 0 |
| | C6-7 | 2413.00 | Silty carbonate rock containing mud | 18.2 | 1.2 | 7.3 | 17.7 | 0 | 0 | 10.4 | 0 |
| | C6-8 | 3667.00 | Silty carbonate rock containing mud | 16.7 | 0.6 | 8.0 | 12.2 | 0 | 0 | 10.1 | 0 |
| Average | C6-10 | 3928.00 | Silty carbonate rock containing mud | 19.0 | 0.7 | 11.2 | 10.9 | 0 | 0 | 9.2 | 0 |
| | | | | 18.5 | 1.1 | 7.9 | 13.6 | 0 | 3.1 | 5.5 | 0 |

Table 2 (continued)

| Name of area | Sample no. | Depth (m) | Designation | Quartz | Potash feldspar | Plagioclase | Calcite | Dolomite | Aragonite | Siderite | Magnesite |
|-------------------|------------|-----------|---|----------|-----------------|-------------|---------|------------|-----------|----------|--------------------------|
| Xianshuiquan area | X9-1 | 1532.95 | Silty dolomite containing mud | 17.7 | 0.9 | 7.5 | 4.5 | 0 | 2.8 | 8.4 | 0 |
| | X9-2 | 1534.40 | Sandy mudstone containing dolomite powder | 23.7 | 1.7 | 6.3 | 7.3 | 0 | 2.6 | 1.0 | 0 |
| | X9-3 | 1536.60 | Sandy mudstone containing dolomite powder | 22.7 | 0.9 | 7.1 | 12.4 | 0 | 2.5 | 0 | 0 |
| | X9-4 | 1537.27 | Dolomite | 7.7 | 0.4 | 2.2 | 15.2 | 0 | 1.9 | 0 | 0 |
| | X9-5 | 1538.67 | Sandy mudstone containing calcite powder | 18.3 | 1.1 | 7.2 | 20.6 | 0 | 1.9 | 1.1 | 0 |
| | X9-6 | 1539.10 | Sandy mudstone containing calcite powder | 21.6 | 1.1 | 10 | 21.1 | 0 | 1.6 | 0.8 | 0 |
| | X9-7 | 1540.80 | Siltstone containing mud | 33.6 | 2.1 | 11.5 | 14.8 | 0 | 1.8 | 0 | 0 |
| | X9-8 | 1541.20 | Dolomitic siltstone containing mud | 26.4 | 6.0 | 6.9 | 11.4 | 0 | 2.0 | 0 | 0 |
| Average | | | | 21.5 | 1.8 | 7.3 | 13.4 | 0 | 2.1 | 1.4 | 0 |
| Name of Area | Halite | Pyrite | Hematite | Analcite | Barite | Anhydrite | Anatase | Glauberite | Augite | Ankerite | Content of Shale content |
| Yuejin area | 0 | 0 | 6.5 | 3.2 | 0 | 0 | 0 | 0 | 0 | 39.0 | 3.1 |
| | 0 | 4.0 | 2.3 | 2.3 | 0 | 0 | 0.5 | 0 | 0 | 51.8 | 12.9 |
| | 0 | 0 | 4.9 | 2.1 | 0 | 0 | 0 | 1.1 | 0 | 64.3 | 10.5 |
| | 0 | 4.2 | 3.5 | 1.9 | 0 | 0 | 2.6 | 0 | 0 | 56.3 | 7.3 |
| | 0.4 | 3.9 | 4.1 | 0 | 0 | 1.1 | 0 | 0 | 0 | 59.4 | 6.4 |
| | 0 | 0 | 5.0 | 1.4 | 0 | 0 | 3.1 | 0 | 0 | 44.3 | 5.8 |
| | 0 | 5.6 | 5.4 | 0 | 0 | 0 | 0.4 | 0 | 0 | 65.2 | 1.9 |
| | 0 | 5.6 | 4.5 | 0 | 0 | 0 | 9.9 | 0 | 0 | 56.6 | 0.9 |
| | 0.6 | 6.4 | 6.1 | 0.8 | 0 | 0 | 0.2 | 0 | 0 | 61.2 | 8.4 |
| | 0 | 7.0 | 4.8 | 1.3 | 0 | 0 | 0 | 0 | 0 | 48.3 | 10.3 |
| 0.1 | 3.7 | 4.7 | 1.3 | 0.0 | 1.7 | 0.1 | 0.1 | 0.3 | 54.6 | 6.8 | |

Table 2 (continued)

| Name of Area | Halite | Pyrite | Hematite | Analcite | Barite | Anhydrite | Anatase | Glauberite | Augite | Ankerite | Content of Shale content |
|-------------------|--------|--------|----------|----------|--------|-----------|---------|------------|--------|----------|--------------------------|
| Yingxi area | 0.6 | 2.9 | 0 | 0 | 0.4 | 0.6 | 0 | 3.1 | 0 | 20.1 | 9.0 |
| | 0.6 | 4.0 | 3.7 | 0 | 0 | 0 | 0.6 | 1.1 | 0 | 41.2 | 8.4 |
| | 2.1 | 4.3 | 3.2 | 0 | 0 | 0 | 0 | 0.8 | 0 | 43.3 | 9.5 |
| | 0.4 | 3.0 | 0 | 0 | 0 | 2.9 | 0 | 1.2 | 0 | 39.2 | 20.3 |
| | 1.2 | 2.9 | 3.6 | 0 | 0 | 10.7 | 0 | 1.3 | 0 | 42.4 | 10.7 |
| | 0.5 | 1.8 | 0 | 0 | 0 | 0.8 | 0 | 4.3 | 0 | 0 | 10.4 |
| | 0 | 3.8 | 0 | 0 | 0 | 16.1 | 0 | 14.0 | 0 | 0 | 9.0 |
| | 0.5 | 4.5 | 3.7 | 0 | 0 | 3.6 | 2.3 | 0 | 3.0 | 51.3 | 12.7 |
| | 0.6 | 2.4 | 0 | 0 | 0 | 4.1 | 0 | 2.8 | 0 | 17.5 | 25.8 |
| | 1.3 | 7.2 | 0 | 0 | 0 | 1.7 | 0 | 3.0 | 0 | 37.3 | 12.3 |
| Ganchaiyou area | 0.8 | 3.7 | 1.4 | 0 | 0 | 4.1 | 0.3 | 3.2 | 0.3 | 29.2 | 12.8 |
| | 0 | 0 | 4.2 | 0 | 0 | 3.9 | 0 | 0 | 0 | 26.1 | 16.7 |
| | 0.4 | 3.6 | 2.2 | 1.7 | 0 | 1.0 | 0 | 0 | 2.5 | 16.7 | 22.7 |
| | 0 | 4.2 | 3.6 | 1.0 | 0 | 1.1 | 0 | 0 | 0 | 28.3 | 20 |
| | 0 | 3.6 | 2.7 | 1.3 | 0 | 2.9 | 0 | 0 | 0 | 15.4 | 19.0 |
| | 0.5 | 2.4 | 2.2 | 1.0 | 0 | 3.7 | 0 | 0 | 0 | 28.4 | 17.5 |
| | 0.5 | 3.2 | 2.3 | 0 | 0 | 3.0 | 0 | 0 | 0 | 17.6 | 18.8 |
| | 0.8 | 2.1 | 0 | 0.5 | 0 | 3.7 | 0 | 0 | 0 | 23.7 | 14.6 |
| | 0 | 4.1 | 0 | 0 | 0 | 4.0 | 0 | 0 | 0 | 29.0 | 15.3 |
| | 0.6 | 2.3 | 0 | 0.8 | 0 | 2.0 | 0 | 0 | 0 | 19.9 | 23.4 |
| | 0.3 | 2.8 | 1.9 | 0.7 | 0 | 2.8 | 0 | 0 | 0.3 | 22.8 | 18.7 |
| Xianshuiquan area | 0 | 0 | 2.7 | 3.0 | 0 | 0.7 | 0 | 0 | 0 | 33.7 | 20.9 |
| | 0.4 | 0 | 0 | 3.5 | 0 | 4.0 | 0 | 0 | 0 | 12.3 | 39.7 |
| | 0 | 1.9 | 0.5 | 3.7 | 0 | 0 | 0 | 0 | 0 | 19.3 | 31.6 |
| | 0 | 0 | 3.2 | 0 | 0 | 0 | 0 | 0 | 0 | 61.3 | 10.1 |
| | 0 | 2.4 | 0.6 | 5.1 | 0 | 1.0 | 0 | 0 | 0 | 0 | 42.6 |
| | 0 | 3.3 | 0 | 5.1 | 0 | 0 | 0 | 0 | 0 | 0 | 37.1 |
| | 0 | 0 | 0 | 3.9 | 0 | 4.0 | 0 | 0 | 0 | 7.2 | 22.9 |
| | 0 | 0 | 1.2 | 2.9 | 0 | 0.8 | 0 | 0 | 0 | 26.5 | 18.0 |
| | 0.1 | 1.0 | 1.0 | 3.4 | 0 | 1.3 | 0 | 0 | 0 | 20 | 27.9 |

lake water is related to the source of carbon, and separately effect between atmospheric CO_2 and dissolved carbon as a function of temperature.

The oxygen isotope change in lacustrine sedimentary system reflects hydrology balanced lakes status, namely the evaporation and injection change. Generally, evaporation makes the $\delta^{18}\text{O}$ in lake water heavier, since the lighter oxygen isotopic molecules escape from the lake surface preferentially, which makes oxygen isotope in carbonate settling in lake water heavier.

The range of $\delta^{13}\text{C}_{\text{PDB}}$ of lacustrine dolomite in Eocene Qaidam basin is between -4.5 and 0.2‰ with an average of -2.4‰ . The range of $\delta^{18}\text{O}_{\text{PDB}}$ is between -6.1 and 0.4‰ with an average of -2.6‰ . Previous research shows typical $\delta^{13}\text{C}_{\text{PDB}}$ lacustrine carbonate rocks is between -2 and 6‰ , and for $\delta^{18}\text{O}_{\text{PDB}}$, it is between -4 and -8‰ . Therefore, it is indicated that the carbon isotopic composition mainly deviates toward the negative and for oxygen isotopic composition toward the positive.

Carbon and oxygen isotope analysis on the carbonate rock in the research area, and compared the analysis results with open lakes (such as the Greifensee Lake in Switzerland, the Henderson Lake in the U.S., and the Huleh Lake in Israel), as well as closed lakes (such as the Great Salt Lake in the North America, and the Turkana Lake and the

Natron-Magadi Lake in Africa), the comparison results indicate that the carbon and oxygen isotopic compositions of carbonate rock setting point in this area is located between open lake and closed lake (Fig. 4), which proves the inference of “semi-closed and semi-opened” confined lacustrine sedimentary environment.

Elemental analysis

Refer to analytical data of trace elements measured with ICP-MS method (Table 3), the Mn/Sr ratio (Wen et al. 2014; Zhou et al. 1997) can be used to evaluate whether the elemental compositions in the existing strata rocks are subject to diagenetic damage as a basis for sample selection with a good preserving effect, the average Mn/Sr ratio is 0.57, mostly less than 3, indicating that the tested samples have not been affected, or only been slightly affected by the diagenesis (Huang et al. 2016b). Therefore, their elemental compositions can reflect the original geochemical information during the sedimentation. Moreover, the correlation coefficient between the Ce abnormal value and the Eu abnormal value can be calculated to 0.02, and the correlation coefficient between the Ce abnormal value and ΣREE is 0.06. Neither of them shows significant correlation, which indicates that the tested samples are affected by the diagenesis

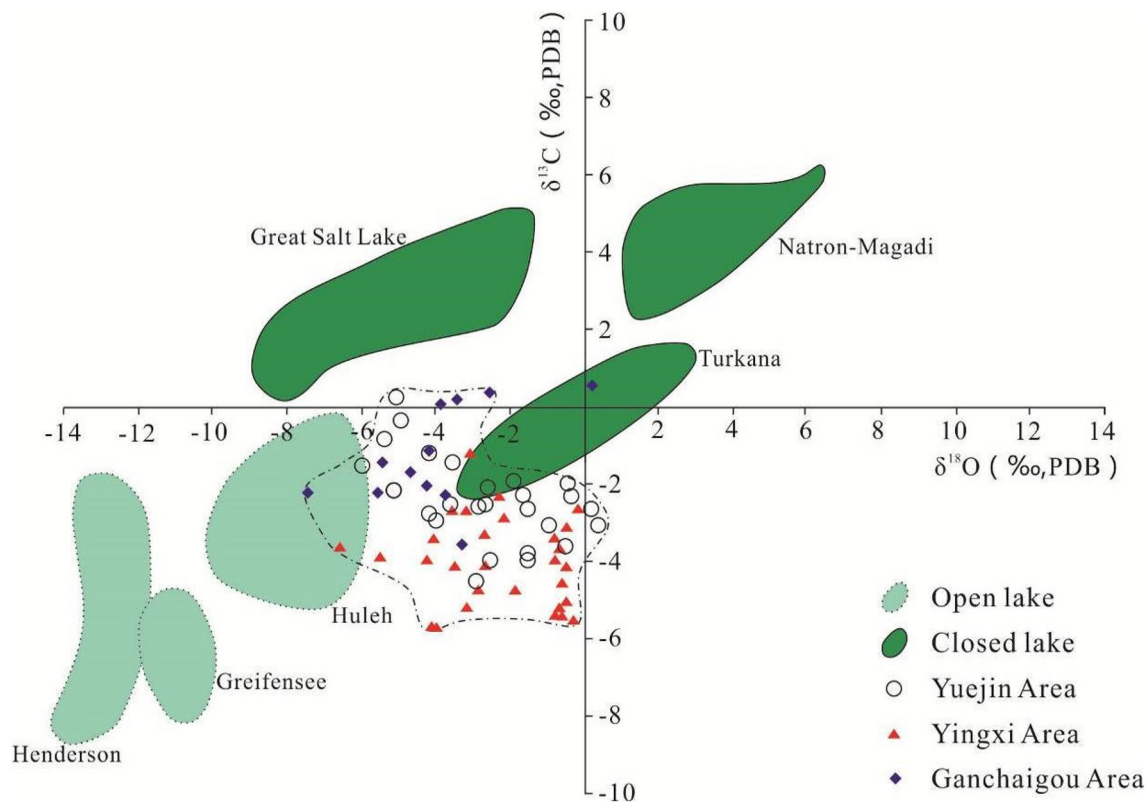


Fig. 4 Carbon and oxygen isotope composition of lacustrine carbonate rocks and analysis of sedimentary environment in Western Qaidam Basin

Table 3 Analysis of trace element geochemistry results list of the E₃ lacustrine dolomite in the Qaidam Basin

| Sample no. | Depth (m) | Lithology | Li | Be | Sc | Ti | V | Cr | Mn | Co | Ni | Cu | Zn | Ga | Ge | |
|------------|-----------|--|-------|--------|-------|---------|--------|-------|--------|---------|-------|-------|--------|-------|-------|------|
| S1-2-8 | 2758.19 | Dolomite containing silt | 30.21 | 1.07 | 4.21 | 1605.41 | 45.50 | 38.91 | 567.34 | 16.12 | 19.57 | 20.29 | 36.50 | 7.64 | 0.51 | |
| S1-2-11 | 2758.52 | Dolomite containing mud | 39.35 | 1.37 | 3.58 | 1780.34 | 53.62 | 40.40 | 498.44 | 9.67 | 21.07 | 25.45 | 56.51 | 9.31 | 0.63 | |
| S203-1 | 1502.70 | Dolomite containing silt | 67.58 | 1.65 | 8.52 | 2321.40 | 66.88 | 60.37 | 617.73 | 16.06 | 27.69 | 23.98 | 32.39 | 13.72 | 0.95 | |
| S203-3 | 4486.40 | Dolomite containing silt | 46.43 | 1.52 | 8.71 | 2444.84 | 81.43 | 61.64 | 461.54 | 30.12 | 31.11 | 26.98 | 162.31 | 16.59 | 1.09 | |
| S203-6 | 4495.35 | Dolomite containing silt | 35.10 | 1.08 | 3.38 | 906.30 | 31.85 | 34.88 | 480.89 | 11.82 | 13.88 | 14.05 | 3.01 | 5.68 | 0.33 | |
| S203-7 | 4496.90 | Dolomite containing silt | 95.55 | 1.91 | 9.63 | 3338.82 | 101.53 | 73.91 | 522.84 | 24.80 | 38.46 | 41.83 | 43.87 | 19.46 | 1.37 | |
| S203-8 | 4500.00 | Silty dolomite | 60.53 | 1.97 | 5.62 | 2442.57 | 73.31 | 54.68 | 637.75 | 24.60 | 28.96 | 29.80 | 51.95 | 13.17 | 0.90 | |
| S23-1 | 4034.90 | Dolomite containing glauberite | 52.37 | 1.65 | 6.74 | 2187.10 | 61.49 | 62.66 | 527.02 | 11.34 | 25.44 | 24.37 | 62.08 | 11.59 | 0.79 | |
| S23-3 | 4173.00 | Dolomite containing calcite | 15.80 | 0.68 | 4.82 | 1084.24 | 26.84 | 29.31 | 332.18 | 6.31 | 12.05 | 10.78 | 22.41 | 4.57 | 0.32 | |
| S25-1 | 4177.50 | Dolomite containing calcite | 13.45 | 0.59 | 2.45 | 581.88 | 31.74 | 38.41 | 414.28 | 8.92 | 10.27 | 6.15 | 50.04 | 3.76 | 0.23 | |
| S25-4 | 4216.80 | Dolomite containing gypsum | 26.59 | 1.26 | 6.02 | 1240.04 | 33.08 | 29.11 | 432.20 | 15.56 | 12.03 | 12.30 | 30.89 | 6.30 | 0.43 | |
| S25-6 | 4221.50 | Dolomite | 13.61 | 1.01 | 2.43 | 601.92 | 25.15 | 37.48 | 414.33 | 4.93 | 7.52 | 5.35 | 9.44 | 3.65 | 0.21 | |
| S30-1 | 4081.00 | Dolomite containing silt | 15.92 | 0.79 | 6.75 | 1498.20 | 35.93 | 38.06 | 477.86 | 11.04 | 15.90 | 11.35 | 31.35 | 6.85 | 0.39 | |
| S32X-6 | 4094.22 | Dolomite containing calcite | 24.85 | 0.70 | 0.85 | 1024.73 | 23.67 | 36.48 | 482.66 | 4.33 | 11.60 | 11.48 | 12.05 | 4.39 | 0.45 | |
| S32X-7 | 4097.74 | Dolomite containing calcite | 30.87 | 0.95 | 2.09 | 1103.61 | 30.07 | 31.02 | 420.56 | 8.38 | 14.12 | 12.45 | 19.28 | 5.56 | 0.58 | |
| S32X-8 | 4100.98 | Silty dolomite containing mud | 49.20 | 1.64 | 5.26 | 1616.63 | 52.93 | 44.72 | 679.77 | 7.92 | 20.11 | 20.55 | 30.85 | 9.88 | 1.12 | |
| S32X-9 | 4102.33 | Argillaceous dolomite containing silt | 35.86 | 1.62 | 9.16 | 2607.42 | 83.84 | 60.90 | 690.83 | 15.22 | 33.53 | 39.51 | 118.01 | 14.05 | 1.75 | |
| S32X-10 | 4112.53 | Sandy limestone containing dolomite powder | 36.86 | 1.30 | 8.91 | 1923.25 | 54.68 | 44.17 | 671.74 | 18.81 | 23.11 | 24.61 | 45.21 | 10.67 | 1.00 | |
| S32X-11 | 4117.04 | Lime stone containing silt | 38.13 | 1.45 | 10.28 | 2292.16 | 80.92 | 58.15 | 507.31 | 13.48 | 31.73 | 24.11 | 51.67 | 14.95 | 1.26 | |
| S32X-12 | 4121.50 | Dolomite containing silt | 20.14 | 1.04 | 4.36 | 1529.52 | 36.99 | 48.21 | 494.68 | 10.07 | 17.02 | 14.55 | 25.57 | 6.17 | 0.58 | |
| S32X-13 | 4127.93 | Dolomite containing calcite | 41.59 | 1.81 | 7.62 | 2177.19 | 79.91 | 86.49 | 661.27 | 12.53 | 30.36 | 25.11 | 61.72 | 14.29 | 1.09 | |
| Sample no. | Rb | Sr | Y | Zr | Nb | Mo | Cd | Sn | Cs | Ba | Hf | Ta | Pb | Bi | Th | U |
| S1-2-8 | 52.68 | 1187.82 | 10.64 | 58.96 | 5.03 | 2.33 | 0.06 | 1.31 | 4.32 | 450.31 | 1.81 | 0.42 | 13.97 | 0.23 | 4.99 | 2.64 |
| S1-2-11 | 65.54 | 3410.48 | 13.05 | 75.99 | 5.47 | 2.34 | 0.08 | 1.55 | 5.59 | 1142.73 | 2.33 | 0.45 | 15.14 | 0.25 | 5.89 | 3.87 |
| S203-1 | 96.92 | 675.05 | 17.05 | 93.09 | 7.46 | 3.19 | 0.06 | 2.15 | 10.25 | 373.52 | 2.70 | 0.56 | 18.91 | 0.29 | 7.77 | 3.70 |
| S203-3 | 100.82 | 1722.24 | 16.19 | 93.88 | 7.59 | 3.94 | 0.63 | 2.33 | 10.61 | 1092.27 | 2.83 | 0.57 | 20.64 | 0.35 | 9.37 | 4.19 |
| S203-6 | 37.07 | 3031.38 | 7.95 | 38.86 | 3.27 | 1.99 | 0.03 | 0.85 | 4.75 | 789.29 | 1.13 | 0.23 | 9.69 | 0.13 | 3.63 | 2.31 |
| S203-7 | 150.63 | 243.76 | 23.88 | 128.90 | 10.59 | 5.82 | 0.06 | 3.31 | 14.97 | 376.62 | 3.90 | 0.83 | 24.84 | 0.47 | 13.27 | 6.57 |
| S203-8 | 102.99 | 460.87 | 18.39 | 97.89 | 8.03 | 2.01 | 0.08 | 2.24 | 8.95 | 392.26 | 2.93 | 0.63 | 26.66 | 0.37 | 8.66 | 3.34 |
| S23-1 | 90.44 | 841.17 | 15.03 | 86.31 | 7.16 | 1.04 | 0.10 | 1.78 | 7.44 | 512.31 | 2.59 | 0.56 | 30.28 | 0.29 | 7.36 | 2.83 |
| S23-3 | 30.95 | 1841.98 | 7.48 | 71.61 | 3.38 | 2.58 | 0.06 | 0.85 | 2.45 | 1213.69 | 1.83 | 0.25 | 7.59 | 0.11 | 3.62 | 1.65 |
| S25-1 | 18.26 | 1771.26 | 6.40 | 24.89 | 1.68 | 2.13 | 0.03 | 0.60 | 1.48 | 1077.57 | 0.68 | 0.14 | 3.15 | 0.08 | 1.56 | 1.53 |
| S25-4 | 32.63 | 1666.25 | 11.17 | 64.95 | 5.01 | 7.51 | 0.08 | 1.20 | 4.58 | 1404.60 | 1.94 | 0.37 | 8.65 | 0.12 | 4.44 | 3.99 |
| S25-6 | 25.62 | 2188.01 | 9.41 | 19.19 | 2.20 | 0.76 | 0.02 | 0.49 | 1.42 | 1333.58 | 0.56 | 0.23 | 5.25 | 0.08 | 2.19 | 1.56 |
| S30-1 | 36.66 | 990.21 | 9.62 | 61.78 | 4.33 | 1.53 | 0.07 | 0.99 | 2.97 | 445.26 | 1.81 | 0.35 | 13.19 | 0.15 | 4.62 | 2.95 |

Table 3 (continued)

| Sample no. | Rb | Sr | Y | Zr | Nb | Mo | Cd | Sn | Cs | Ba | Hf | Ta | Pb | Bi | Th | U |
|------------|-------|---------|-------|--------|------|------|------|------|------|---------|------|------|-------|------|------|------|
| S32X-6 | 29.04 | 1061.46 | 7.36 | 30.52 | 4.07 | 2.25 | 0.03 | 0.91 | 2.82 | 599.97 | 0.87 | 0.33 | 7.27 | 0.10 | 2.04 | 1.73 |
| S32X-7 | 32.70 | 2629.72 | 7.66 | 41.13 | 3.35 | 2.13 | 0.05 | 0.91 | 3.04 | 590.07 | 1.17 | 0.28 | 9.21 | 0.14 | 3.41 | 1.72 |
| S32X-8 | 66.52 | 1539.85 | 14.59 | 67.92 | 5.01 | 5.16 | 0.05 | 3.29 | 6.54 | 782.59 | 2.03 | 0.40 | 10.13 | 0.19 | 6.20 | 4.41 |
| S32X-9 | 82.83 | 546.94 | 20.53 | 115.35 | 8.02 | 6.87 | 0.21 | 2.58 | 8.69 | 539.78 | 3.45 | 0.66 | 25.15 | 0.40 | 9.92 | 9.56 |
| S32X-10 | 66.10 | 1410.86 | 16.52 | 95.06 | 5.98 | 5.26 | 0.06 | 1.47 | 7.21 | 762.36 | 2.76 | 0.50 | 15.23 | 0.23 | 7.72 | 4.50 |
| S32X-11 | 91.18 | 1755.76 | 17.09 | 90.42 | 6.59 | 6.28 | 0.06 | 2.24 | 9.86 | 821.41 | 2.63 | 0.52 | 17.00 | 0.30 | 7.64 | 4.93 |
| S32X-12 | 41.67 | 603.86 | 10.10 | 89.66 | 5.12 | 3.10 | 0.06 | 1.00 | 3.31 | 227.55 | 2.58 | 0.40 | 12.53 | 0.19 | 5.17 | 2.84 |
| S32X-13 | 95.78 | 1982.75 | 16.27 | 85.46 | 6.50 | 6.31 | 0.07 | 2.10 | 9.35 | 1134.32 | 2.56 | 0.50 | 16.67 | 0.29 | 7.58 | 4.46 |

The data of average UCC values of trace elements are cited from the research result data of Taylor and Mclenan

to a very limited extent, and the tested samples are able to represent the fluids geochemical characteristics during the sedimentation. It can be seen from the standardized spider web diagram (Fig. 5) of average upper continental crust (UCC) trace elements values (Taylor and Mclenan 1985) in dolomite obtained from the research area that Sr, Mo, Cs and Bi are subject to significant enrichment, and Nb, Sn and Ta contents are obviously lower than the average UCC values, Sr elements (in a high content) are the products sedimented at the saline lake basin, the celestite (SrSO_4) minerals presenting a high brightness can be obviously seen in the SEM back-scattered color images.

The Sr/Ba ratio is generally used for evaluating the sedimentation environment of lake water (Deng and Qian 1993), under the principle that the freshwater lake has less sulfate ions, so the sedimentations of Sr and Ba are unlikely to occur as the lake water gradually salinizes; The degree of mineralization gradually increases, the sedimentation of BaSO_4 will occur firstly, followed gradually by sedimentation of SrSO_4 , therefore, have the higher the Sr/Ba ratio in the sediment, the higher the degree of salinization; the Sr content minimum value is 243.76 ppm. 21 samples obtained from in research area, the maximum value is 3410.48 ppm with an average of 1502.94 ppm; the Ba content ranges from 227.55 to 1404.60 ppm with an average of 764.86 ppm; the Sr/Ba ratio is greater than 1 with an average of 2.01. Therefore, it can be considered as typical saline lake sedimentation. Some scholars analysis on correlation between Sr/Ba ratio and elements B and Cl (the two indicating elements of salinity), obtained a no correlation conclusion, and a good positive correlation (Sun et al. 1997) between Sr/Ba ratio and carbonate content. Therefore, the sediment carbonate would affect the Sr/Ba ratio, so this ratio could not correctly reflect the original Sr/Ba ratio, such as Sr, paleosalinity of sedimentation environment might easily intrude into carbonate to replace a little Ca, the ratio was primarily controlled by Sr distribution coefficient in the carbonate. As a result, a little Sr existing would bring a certain error on paleosalinity estimate. For the research samples obtained from this area, an analysis on correlation between the Sr/Ba ratio measured with the ICP-MS method and the carbonate content measured by XRD (Fig. 6), indicates a relatively poor correlation (the correlation coefficient being only 0.18). The carbonate can only slightly affect the Sr/Ba ratio; therefore, it can be basically confirmed that using the Sr/Ba ratio as an indicator for a saline lake sedimentation environment in the research area is a relatively accurate method.

The Sr/Cu ratio is relatively sensitive to paleoclimate, and it is generally recognized that the Sr/Cu ratio is greater than the limit value 5 indicating an arid climate (Li and Zhou 2015). However, the Sr/Cu ratio calculated with the research samples is 5.83 ~ 408.92 with an average of 109.04, much higher than the limit value 5. Therefore,

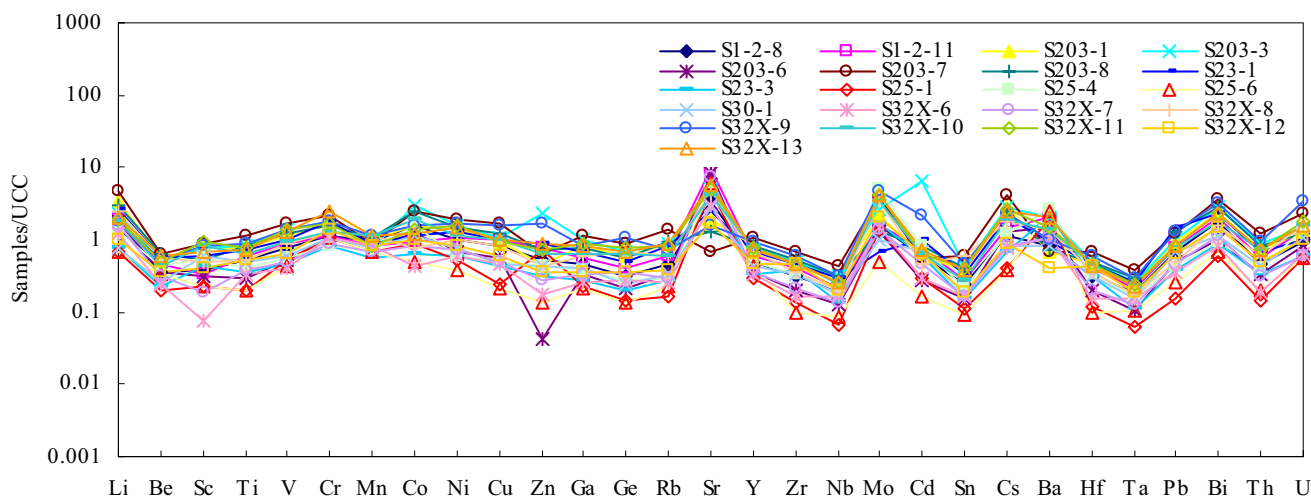


Fig. 5 Average standardized upper crust discrete rare element's spider web of the E₃² lacustrine dolomites in Western Qaidam Basin

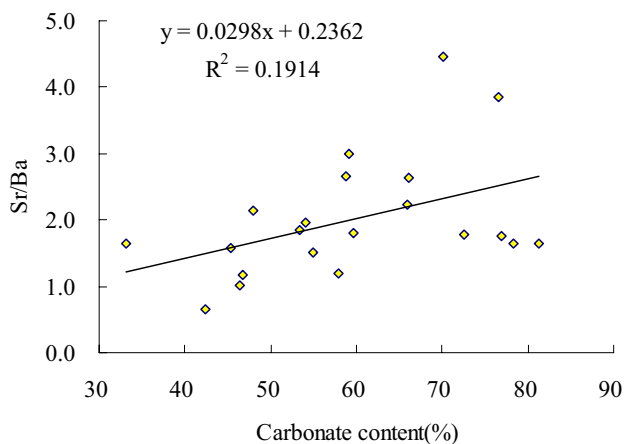


Fig. 6 Correlation between the carbonate content and Sr/Ba ratio of the E₃² reservoirs in Western Qaidam Basin

it indicates an arid climate, which is consistent with the evaporitic environment reflected by relatively developed saline minerals in the petrological characteristics. The U/Th ratio is able to reflect the oxygen-rich characteristics and oxygen-poor characteristics in the sedimentation environment. It is generally recognized that this ratio greater than 1 indicates an oxygen-rich environment, and this ratio less than 1 indicates an oxygen-poor environment. The U/Th ratio is 0.38~0.98, with an average of 0.62, completely lower than the limit value 1. Therefore, it indicates an oxygen-poor reducing environment. δ Ce is distributed in a range of 0.98~1.02 with an average of 1.01, basically with no anomaly, which indicates that the sedimentation occurs in the reducing sedimentation environment (Li and Zhou 2015).

Rare earth element

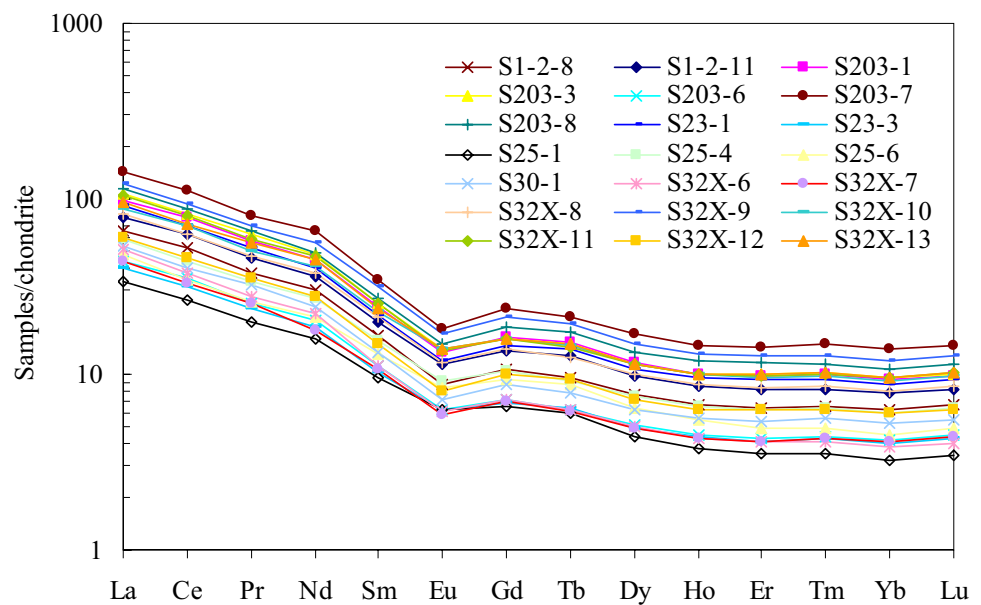
The analytical data obtained from the analysis on rare earth elements measured with the ICP-MS method (Table 4), total average quantity of the rare earth elements is 87.67 ppm (39.41~162.67 ppm), obtained from the lacustrine dolomite samples in the Qaidam Basin, between the chondrite Σ REE value (2.56 ppm) and average UCC Σ REE value (146.37 ppm) (Li and Zhou 2015). Generally, total quantity of the rare earth elements in the carbonate rocks accounts for a relatively low proportion in sedimentary rocks, mostly lower than 100 ppm (Wang 1989), some only being 20~30 ppm (Li and Zhou 2015). Hydrothermal dolomite also occupies a low content of rare earth elements. A few samples with extremely low quantity rare earth elements (such as 39.41 ppm) may have hydrothermal traces at some places (Kucera et al. 2009; Tang et al. 2013). Some samples with relatively high quantity of rare earth elements (such as 162.67 ppm) may be related to the mixed terrigenous clastics represented by fine-grained clay minerals, which in most cases enrich rare earth elements (Henderson 1984), thereby increasing the total rare earth elements quantity the entire rock to a certain extent. The rare earth elements distribution pattern diagram indicates a low-medium Eu negative anomaly (Fig. 7), and it is generally recognized that this is closely related to the interference by upper continental crust. It is affected by shale content mixed in the lacustrine dolomite to a certain extent, the Eu negative anomaly existence and the Eu positive anomaly missing in most samples indicate that the mantle-derived fluids have not involved the dolomite sedimentation in a large scale. Numerous previous research results have also proved that the research area is the penecontemporaneous metasomatic genesis (Cao et al. 2014; Yin et al. 2007; Sun et al. 2005), and the average

Table 4 Analysis of REE results list of the Eocene lacustrine dolomite in Western Qaidam Basin

| Sample no. | Lithology | Depth (m) | La | Ce | Pr | Nd | Sm | Eu | Gd | Tb | Dy | Ho | |
|------------|-----------|--|-------|-------|--------|--------|-------|-----------|---------|---------|---------|------|------|
| S1-2-8 | 2758.19 | Dolomite containing silt | 15.61 | 32.07 | 3.61 | 14.25 | 2.57 | 0.51 | 2.21 | 0.36 | 1.95 | 0.38 | |
| S1-2-11 | 2758.52 | Dolomite containing mud | 18.78 | 38.05 | 4.42 | 16.88 | 3.03 | 0.67 | 2.79 | 0.47 | 2.46 | 0.48 | |
| S203-1 | 4502.70 | Dolomite containing silt | 23.29 | 47.45 | 5.51 | 20.84 | 3.72 | 0.78 | 3.35 | 0.57 | 2.94 | 0.57 | |
| S203-3 | 4486.40 | Dolomite containing silt | 25.32 | 50.55 | 5.95 | 22.47 | 3.87 | 0.81 | 3.30 | 0.56 | 2.91 | 0.57 | |
| S203-6 | 4495.35 | Dolomite containing silt | 10.52 | 21.50 | 2.39 | 9.51 | 1.71 | 0.36 | 1.48 | 0.24 | 1.29 | 0.25 | |
| S203-7 | 4496.90 | Dolomite containing silt | 33.72 | 68.49 | 7.68 | 30.65 | 5.24 | 1.05 | 4.82 | 0.80 | 4.29 | 0.82 | |
| S203-8 | 4500.00 | Silty dolomite | 27.03 | 53.70 | 6.30 | 23.00 | 4.15 | 0.86 | 3.80 | 0.65 | 3.42 | 0.67 | |
| S23-1 | 4034.90 | Dolomite containing glauberite | 21.72 | 42.68 | 5.01 | 18.75 | 3.34 | 0.70 | 3.03 | 0.52 | 2.72 | 0.54 | |
| S23-3 | 4173.00 | Dolomite containing calcite | 9.65 | 19.17 | 2.25 | 8.74 | 1.56 | 0.37 | 1.41 | 0.24 | 1.25 | 0.25 | |
| S25-1 | 4177.50 | Dolomite containing calcite | 8.01 | 16.19 | 1.90 | 7.36 | 1.45 | 0.36 | 1.36 | 0.23 | 1.12 | 0.21 | |
| S25-4 | 4216.80 | Dolomite containing gypsum | 13.91 | 27.27 | 3.22 | 12.56 | 2.38 | 0.53 | 2.13 | 0.35 | 1.88 | 0.37 | |
| S25-6 | 4221.50 | Dolomite | 11.33 | 21.37 | 2.44 | 9.97 | 2.01 | 0.48 | 1.94 | 0.33 | 1.63 | 0.31 | |
| S30-1 | 4081.00 | Dolomite containing silt | 12.66 | 24.81 | 3.06 | 11.29 | 2.05 | 0.42 | 1.79 | 0.29 | 1.61 | 0.32 | |
| S32X-6 | 4094.22 | Dolomite containing calcite | 12.25 | 23.06 | 2.62 | 10.46 | 1.72 | 0.36 | 1.47 | 0.23 | 1.27 | 0.25 | |
| S32X-7 | 4097.74 | Dolomite containing calcite | 10.36 | 20.28 | 2.40 | 8.39 | 1.64 | 0.34 | 1.44 | 0.23 | 1.25 | 0.24 | |
| S32X-8 | 4100.98 | Silty dolomite containing mud | 19.22 | 38.26 | 4.52 | 17.81 | 3.26 | 0.68 | 2.89 | 0.47 | 2.53 | 0.50 | |
| S32X-9 | 4102.33 | Argillaceous dolomite containing silt | 29.16 | 57.79 | 6.73 | 26.29 | 4.81 | 0.99 | 4.35 | 0.73 | 3.81 | 0.74 | |
| S32X-10 | 4112.53 | Sandy limestone containing dolomite powder | 20.88 | 42.79 | 4.83 | 19.23 | 3.47 | 0.80 | 3.26 | 0.55 | 2.87 | 0.56 | |
| S32X-11 | 4117.04 | Lime stone containing silt | 24.89 | 49.21 | 5.62 | 21.98 | 3.92 | 0.79 | 3.31 | 0.53 | 2.89 | 0.57 | |
| S32X-12 | 4121.50 | Dolomite containing silt | 14.13 | 27.96 | 3.32 | 12.95 | 2.28 | 0.47 | 2.08 | 0.35 | 1.82 | 0.36 | |
| S32X-13 | 4127.93 | Dolomite containing calcite | 22.78 | 43.80 | 5.29 | 21.24 | 3.59 | 0.81 | 3.27 | 0.56 | 2.88 | 0.57 | |
| Sample no. | Er | Tm | Yb | Lu | ΣREE | LREE | HREE | LREE/HREE | LaN/YbN | LaN/SmN | GdN/YbN | δEu | δCe |
| S1-2-8 | 1.07 | 0.17 | 1.06 | 0.17 | 75.83 | 68.63 | 7.37 | 9.31 | 10.60 | 3.92 | 1.73 | 0.65 | 1.05 |
| S1-2-11 | 1.37 | 0.21 | 1.32 | 0.21 | 90.93 | 81.83 | 9.31 | 8.79 | 10.19 | 4.00 | 1.75 | 0.70 | 1.02 |
| S203-1 | 1.63 | 0.26 | 1.60 | 0.25 | 112.52 | 101.61 | 11.17 | 9.10 | 10.44 | 4.04 | 1.73 | 0.67 | 1.03 |
| S203-3 | 1.64 | 0.26 | 1.62 | 0.25 | 119.83 | 108.97 | 11.12 | 9.79 | 11.19 | 4.23 | 1.68 | 0.70 | 1.01 |
| S203-6 | 0.72 | 0.11 | 0.71 | 0.11 | 50.79 | 45.99 | 4.92 | 9.35 | 10.60 | 3.97 | 1.72 | 0.69 | 1.05 |
| S203-7 | 2.36 | 0.38 | 2.37 | 0.37 | 162.67 | 146.84 | 16.21 | 9.06 | 10.21 | 4.15 | 1.68 | 0.64 | 1.04 |
| S203-8 | 1.94 | 0.29 | 1.83 | 0.29 | 127.65 | 115.03 | 12.91 | 8.91 | 10.57 | 4.21 | 1.71 | 0.66 | 1.01 |
| S23-1 | 1.55 | 0.24 | 1.49 | 0.24 | 102.29 | 92.19 | 10.33 | 8.92 | 10.44 | 4.20 | 1.68 | 0.67 | 1.00 |
| S23-3 | 0.69 | 0.11 | 0.68 | 0.11 | 46.36 | 41.74 | 4.73 | 8.82 | 10.17 | 3.99 | 1.71 | 0.76 | 1.01 |
| S25-1 | 0.58 | 0.09 | 0.55 | 0.09 | 39.41 | 35.27 | 4.22 | 8.35 | 10.45 | 3.55 | 2.05 | 0.79 | 1.02 |
| S25-4 | 1.04 | 0.16 | 1.02 | 0.16 | 66.83 | 59.87 | 7.12 | 8.41 | 9.80 | 3.77 | 1.73 | 0.72 | 1.00 |
| S25-6 | 0.82 | 0.13 | 0.77 | 0.12 | 53.51 | 47.60 | 6.04 | 7.88 | 10.55 | 3.64 | 2.08 | 0.75 | 1.00 |
| S30-1 | 0.89 | 0.14 | 0.89 | 0.14 | 60.22 | 54.29 | 6.07 | 8.94 | 10.22 | 3.99 | 1.67 | 0.66 | 0.98 |
| S32X-6 | 0.68 | 0.11 | 0.65 | 0.10 | 55.11 | 50.46 | 4.75 | 10.62 | 13.46 | 4.60 | 1.86 | 0.68 | 1.00 |
| S32X-7 | 0.69 | 0.11 | 0.70 | 0.11 | 48.09 | 43.42 | 4.78 | 9.09 | 10.68 | 4.08 | 1.71 | 0.68 | 1.00 |
| S32X-8 | 1.37 | 0.22 | 1.36 | 0.22 | 93.05 | 83.73 | 9.54 | 8.78 | 10.16 | 3.81 | 1.76 | 0.68 | 1.01 |
| S32X-9 | 2.13 | 0.33 | 2.03 | 0.32 | 139.88 | 125.78 | 14.43 | 8.71 | 10.32 | 3.91 | 1.77 | 0.66 | 1.01 |
| S32X-10 | 1.60 | 0.25 | 1.55 | 0.25 | 102.63 | 92.00 | 10.88 | 8.45 | 9.65 | 3.88 | 1.74 | 0.73 | 1.04 |
| S32X-11 | 1.61 | 0.26 | 1.62 | 0.26 | 117.18 | 106.41 | 11.03 | 9.64 | 11.04 | 4.10 | 1.69 | 0.67 | 1.02 |
| S32X-12 | 1.03 | 0.16 | 1.02 | 0.16 | 67.94 | 61.11 | 6.99 | 8.75 | 9.92 | 4.01 | 1.68 | 0.66 | 1.00 |
| S32X-13 | 1.64 | 0.26 | 1.63 | 0.26 | 108.30 | 97.50 | 11.06 | 8.82 | 10.04 | 4.09 | 1.66 | 0.73 | 0.98 |

The standardized data of chondrite of rare earth elements are cited from the research results data of Sun and McDonough. ΣREE is the total content of rare earths; LREE/HREE is the ratio of light rare earths to heavy rare earths (LREE represents light rare earths, while HREE represents heavy rare earths); $(La/Yb)_N$, where N represents the ratio upon standardization of chondrite data; $\delta Eu = (Eu)_N / \sqrt{(Sm \times Gd)_N}$; $\delta Ce = (Ce)_N / \sqrt{(La \times Pr)_N}$, where N represents the value upon standardization of chondrite data

Fig. 7 REE distribution patterns of the E_3^2 lacustrine dolomites in Western Qaidam Basin



values of LREE/HREE, $(La/Yb)_N$, $(La/Sm)_N$ and $(Gd/Yb)_N$ are, respectively, 8.98, 10.51, 4.01 and 1.75. It is indicated that the light and heavy rare earths in the lacustrine dolomite are subject differentiation, and that the light rare earths more differentiated than the heavy rare earths. All distribution curves of rare earths are rightward, and heavy rare earths correspond to a relatively flat curve. This distribution model and characteristics reflect the mixed genesis characteristics, the rocks include multiple types of mineral compositions and multiple types of material sources.

Conclusions

Micritic lacustrine carbonate rocks are primarily developed in Oligocene E_3^2 in the Qaidam Basin; however, Yuejin area, Yingxi area, Ganchaigou area and Xianshuiquan area are subject to a certain difference in petrological characteristics: Yuejin area and Yingxi area have the highest carbonate contents, Xianshuiquan area and Ganchaigou area have the highest contents of terrigenous clastics, Xianshuiquan Area has the highest shale content, and Yingxi Area has the highest content of saline minerals. These petrographic characteristics are mainly controlled by the sedimentary environments.

Yingxi area is a semi-closed and semi-open lacustrine saline sedimentary environment, primarily influenced by: lithologic characteristics dominated by dark colors such as dark gray or black, and mixed with saline minerals sedimentation; palaeogeomorphologic characteristics prior to sedimentation in E_3^2 ; carbon and oxygen isotopes compositions; various trace elements such as Sr/Ba ratio, Sr/Cu ratio and U/Th ratio; distribution pattern of rare earth elements.

Acknowledgements This study is financially supported by National Major Project of science and technology in developing great oil&gas field and coal bed gas (2016ZX05007-006), Study on water-cut control and production stabilization in the old gasfields and efficient development in new gasfields, in Qaidam Basin (2016E-0106GF). The authors also thank the anonymous reviewers for their constructive comments and the editorial staff for their diligent work.

References

- Cao Z, Wei Z, Lin C (2014) The kinetics of oil generation in a saline basin: a case study of the source rock of tertiary in Zhahaquan Depression, Qaidam Basin, China. *Pet Sci Technol* 32(21):2648–2657. <https://doi.org/10.1080/10916466.2014.913623>
- Deng H, Qian K (1993) Sedimentary geochemistry and environmental analysis. Gansu Science and Technology Press, Lanzhou, pp 18–31
- Henderson P (1984) Rare earth element geochemistry. Elsevier, Amsterdam, pp 52–71
- Huang C, Yuan X, Wu L (2016a) Origin of continental facies dolomite and research methods in lacustrine basin. *Lithol Reserv* 38(1):7–15
- Huang C, Yuan J, Tian G (2016b) The geochemical characteristics and formation mechanism of the Eocene lacustrine dolomite reservoirs in the Qaidam. *Earth Sci Front* 23(3):510–521
- Huang C, Yuan X, Song C (2017) Characteristics, origin, and role of salt minerals in the process of hydrocarbon accumulation in the saline lacustrine basin of the Yingxi Area, Qaidam, China. *Carbonates Evaporites* 2017:1–16. <https://doi.org/10.1007/s13146-017-0350-9>
- Jia C (2005) Foreland thrust-fold belt features and gas accumulation in Midwest China. *Pet Explor Dev* 32(2):1–9
- Kucera J, Cempípek J, Dolníček Z (2009) Rare earth elements and yttrium geochemistry of dolomite from post-Variscan vein-type mineralization of the Nizky Jeseník and Upper Silesian Basins, Czech Republic. *J Geochem Explor* 103:69–79
- Li X, Zhou Y (2015) Geochemical characteristics of trace elements and their implications for the Xiayuangong ore section of Fengcun

- lead-zinc deposits in Qingzhou-Hangzhou metallogenic belt. *Earth Sci Front* 22(2):131–143
- Mao L, Yi H, Ji C (2014) Petrography and carbon-oxygen isotope characteristics of the Cenozoic lacustrine carbonate rocks in Qaidam Basin. *Geol Sci Technol Inf* 33(1):41–48 (**in Chinese**)
- Peng C (2011) Distribution of favorable lacustrine carbonate reservoirs: a case from the Upper Es4 of Zhanhua Sag, Bohai Bay Basin. *Pet Explor Dev* 38(4):435–443 (**in Chinese**)
- Sun Z, Yang F, Zhang Z (1997) Sedimentary environments and hydrocarbon generation of cenozoic salified lakes in China. Petroleum Industry Press, Beijing, pp 125–142
- Sun Z, Yang Z, Pei J (2005) Magnetostratigraphy of Paleogene sediments from northern Qaidam basin, China: implications for tectonic uplift and block rotation in northern Tibetan plateau. *Earth Planet Sci Lett* 237:635–646. <https://doi.org/10.1016/j.epsl.2005.07.007>
- Tang H, Chen Y, Santosh M (2013) REE geochemistry of carbonates from the Guanmenshan Formation, Liaohe Group, NE Sino-Korean Craton: implications for seawater compositional change during the Great Oxidation Event. *Precambrian Res* 227:316–336
- Taylor R, Mclenan SM (1985) The continental crust: its composition and evolution. Blackwell, London, pp 57–72
- Tuo J, Huang X (1996) Advances on lacustrine carbonate source rocks research. *Adv Earth Sci* 11(6):585–589 (**in Chinese**)
- Tuo J, Shao H, Huang X (1995) Lacustrine carbonate source rocks and their organic geochemical characteristics: taking the Tertiary system of Qaidam Basin as an example. *Exp Pet Geol* 17(3):272–276 (**in Chinese**)
- Wang Z (1989) Geochemistry of rare earth element. Science Press, Beijing
- Wen H, Zheng R, Qing H (2014) Primary dolostone related to the Cretaceous lacustrine hydrothermal sedimentation in Qingxi sag, Jiuquan Basin on the northern Tibetan Plateau. *Sci China Earth Sci* 44(4):591–604
- Xia Zhu (1986) Structure of petroliferous basins in China. Petroleum Industry Press, Beijing (**in Chinese**)
- Xia Q, Tian J, Ni X (2003) Lacustrine carbonate rocks in China: an overview. *Sediment Geol Tethyan Geol* 23(1):105–112 (**in Chinese**)
- Yin A, Dang Y, Zhang M (2007) Cenozoic tectonic evolution of Qaidam basin and its surrounding regions. *Geol Soc Am Spec Pap* 433:369–390. [https://doi.org/10.1130/2007.2433\(18\)](https://doi.org/10.1130/2007.2433(18))
- You X, Sun S, Zhu J (2011) Progress in the study of microbial dolomite model. *Earth Sci Front* 18(4):52–64
- Zhao F (2013) Lacustrine algal limestone reservoir in Qaidam Basin, China. *Carbonates Evaporites* 1:2–8. <https://doi.org/10.1007/s13146-013-0182-1>
- Zhao F (2014) Identification of Neogene mixed lacustrine carbonate in Qaidam basin. *Carbonates Evaporates*. <https://doi.org/10.1007/s13146-014-0210-9>
- Zhou S, Jester V, Pulater N (1991) The lake sedimentary system and oil and gas. Science Press, Beijing, pp 81–113 (**in Chinese**)
- Zhou C, Zhang J, Li G (1997) Carbon and oxygen isotopic record of the early Cambrian from the Xiaotan Section, Yunnan, South China. *Chin J Geol* 32(2):201–211

Publisher's Note Springer Nature remains neutral with regard to jurisdictional claims in published maps and institutional affiliations.